Tribology Letters (2019) 67:46
https://doi.org/10.1007/s11249-019-1158-7

ORIGINAL PAPER

How Sliding and Hydrodynamics Contribute to Articular Cartilage Fluid and Lubrication Recovery

D. L. Burris[1,2] · L. Ramsey[3] · B. T. Graham[2] · C. Price[1,2] · A. C. Moore[1,4]

Received: 7 December 2018 / Accepted: 19 March 2019 / Published online: 2 April 2019

Abstract

The tribological functions of cartilage are governed primarily by its interstitial fluid content, but the means by which cartilage recovers and retains interstitial fluid during articulation following periods of static loading remain unclear. Recently, we demonstrated a phenomenon in which articular cartilage recovers fluid at the loaded contact interface; we refer to this as 'tribological rehydration'. Our findings were consistent with two competing hypotheses: (1) that hydrodynamic pressures exceeded local interstitial pressures; (2) that fluid from the trailing wedge squeezed into the porous surface during direction reversals (reciprocal wedging). In this paper, we use unidirectional sliding to eliminate the potential effects of reciprocal wedging on tribological rehydration. We observed the same tribological rehydration effects from speed as in our previous reciprocating studies; thus, any effects of reciprocation are secondary to those of sliding itself. Tribological rehydration was enhanced by increased speeds, decreased loads, increased lubricant viscosity, and increased sample diameter. Although our results are generally consistent with a hydrodynamic interpretation of tribological rehydration, our attempts to eliminate the convergence zone by systematically decreasing the sample diameter failed to extinguish tribological rehydration. This final observation reveals an extremely robust mechanism for preventing tissue collapse and highlights some of the remaining challenges in modeling cartilage as a mechanical and tribological material.

Keywords Cartilage · Hydration · Lubrication · Hydrodynamics · Tribological rehydration

1 Introduction

Articular cartilage is the biological bearing material responsible for load support and lubrication of mammalian joints. The most important functions of articular cartilage, which include lubrication [1–4]), pressurization of interstitial fluid [1, 5–7], mechanical stiffness [5, 8–11], load support [1, 5–7, 12], and stress shielding [12–14], are fundamentally related to the hydration state of the tissue. Although cartilage water content is usually described as a fixed material property on the order of 80%, it is well documented that water content (tissue thickness) is lost during loading [4, 8, 15–19].

McCutchen first measured the fluid exudation process using controlled explant experiments more than 50 years ago and showed that the loss of sample thickness via fluid exudation led to proportionally increased friction over time [1]. Biphasic modeling, pioneered by Mow and colleagues [20, 21], has shown that the load-induced exudation response of cartilage is fundamentally the same as that of other porous materials like rocks, soils, sponges, and hydrogels; loading necessarily pressurizes the incompressible interstitial fluid, which subsequently flows toward low pressure outside the porous media according to Darcy's Law.

While the exudation response of cartilage to static loading is well studied, the rehydration process is less clear. One well-known mechanism for fluid recovery is based on the density of the fixed charges within the tissue. These fixed charges set up an osmotic stress that creates a driving force

Electronic supplementary material The online version of this article (https://doi.org/10.1007/s11249-019-1158-7) contains supplementary material, which is available to authorized users.

✉ A. C. Moore
axel.moore@imperial.ac.uk

[1] Department of Biomedical Engineering, University of Delaware, Newark, DE, USA

[2] Department of Mechanical Engineering, University of Delaware, Newark, DE, USA

[3] Avon Grove High School, West Grove, PA, USA

[4] Department of Bioengineering, Imperial College London, Royal School of Mines, London SW7 2AZ, UK

for rehydration when the cartilage is unloaded [19, 21–23]. In vivo studies of the human knee have shown that recovery rates due to joint unloading are on the order of a few percent per hour [19, 24] and that the strains accumulated each day are reversed each night [23]. During the active part of the day, when joints are frequently loaded, tissue strains due to load-induced fluid exudation are large and accumulate quickly (e.g., ~ 50% strain in 90 min) [15, 19, 24]. However, strains in the human knee at the end of the day remain below ~ 5% [23], suggesting additional modes of fluid recovery. Eckholm and Inglemark found that mammalian joints recovered thickness during articulation [17, 25–27]; this observation implies a motion-induced recovery mode. In situ measurements by Linn on dog ankles again demonstrated this articulation-induced recovery effect; the recovery from static unloading was slower than that from loaded articulation and many times slower than that from unloaded articulation [28]. Linn concluded that articulation periodically exposed the dehydrated zones to the bath, which enabled rapid free swelling and net fluid recovery even during loaded articulation. Until recently, activity-induced fluid recovery and retention has been attributed entirely to the migratory nature of our joints [4, 7, 12, 13].

A few years ago, however, we used in situ strain and solute transport measurements to demonstrate that cartilage can actively recover interstitial hydration during sliding within a constantly loaded stationary contact area that precludes any possible contribution from contact migration [29–31]; we called the phenomenon 'tribological rehydration' to reflect the fact that recovery was induced by sliding. While existing theories fail to explain the tribological rehydration phenomenon, our results are consistent with hydrodynamic origins. Furthermore, a hydrodynamic interpretation appears physically plausible given the large body of theoretical research indicating that significant hydrodynamic pressures do develop within joints and significantly affect their tribological behaviors [32–35].

Although the observation of tribological rehydration has provided new and important insights into how joints recover and retain interstitial fluid, nutrients, and mechanical functions, it remains uncertain if tribological rehydration is primarily sliding-induced. Recent observations from Bonnevie et al. [36], for example, pave the grounds for an alternate hypothesis. They showed that cartilage produces a significant 'wedge' at the trailing edge of contact; the squeeze-film effect from the closing of this wedge during sliding reversals can be expected to produce a rehydration effect that depends on the frequency of reversal and, thus, sliding speed in fixed track-length experiments. Since all of our previous studies involved reciprocation, it is impossible to distinguish between the contributions from sliding and the reversals. Our first objective in this paper was to isolate the contribution of sliding alone by eliminating reciprocal wedging with unidirectional sliding. Our second objective was to determine how hydrodynamic factors, namely, speed, load, lubricant composition, and contact geometry, contribute to the tribological rehydration of cartilage.

2 Methods

2.1 Specimen Preparation

Mature bovine stifle joints were obtained from a local butcher (Herman's Quality Meats, Newark, DE). Joints were disarticulated, and 48 (19 mm diameter) osteochondral cores were extracted along the central region of the lateral and medial sides of 17 femoral condyles. The tissue cores included ~ 1.5 mm of articular cartilage attached to ~ 10 mm of subchondral bone. Samples were washed to remove excess debris (care was taken to not contact the cartilage surface) and were then stored in 1X phosphate buffered saline (PBS) (21-040-CM, Mediatech) at 4 °C or dried under rough vacuum for 24 + hours to preserve the tissue. The dried cartilage served two purposes in this study: (1) it prevented degradation of the tissue during extended periods of storage and (2) it shows that tribological rehydration is persevered following dehydration, which demonstrates robustness. Previous work by several authors have shown that tissue dehydration is an effective method of preserving cartilage mechanics [1, 29, 37].

Prior to testing, dehydrated samples were rehydrated in PBS overnight at 4 °C. Samples were then allowed to warm to room temperature before loading them on the rotary pin-on-disc tribometer shown in Fig. 1. The cartilage explant was submerged in PBS and loaded against a rotating glass disk. The center of the sample was located 21 mm from the rotational axis of the spindle; the sliding speed for a point contact is the product of the measured radius (21 mm) and angular velocity. It is important to note that a 19-mm-diameter cartilage sample loaded to 5 N produces a contact diameter on the order of 5 mm; this leads to a speed variation of ± 12% across the contact. All reported sliding speeds represent the mean sliding speed. Normal and frictional forces were measured with a six-channel load cell (Nano17, ATI Industrial Automation). A vertical nano-positioning stage (P-628, Physik Instrumente) with an internal capacitive displacement sensor was used to control load and measure the deformation/recovery response of the sample. The uncertainties of the displacement sensor and normal force are 20 nm and 5 mN, respectively.

2.2 Preconditioning

Each sample underwent a preconditioning exercise immediately prior to tribological testing to effectively normalize

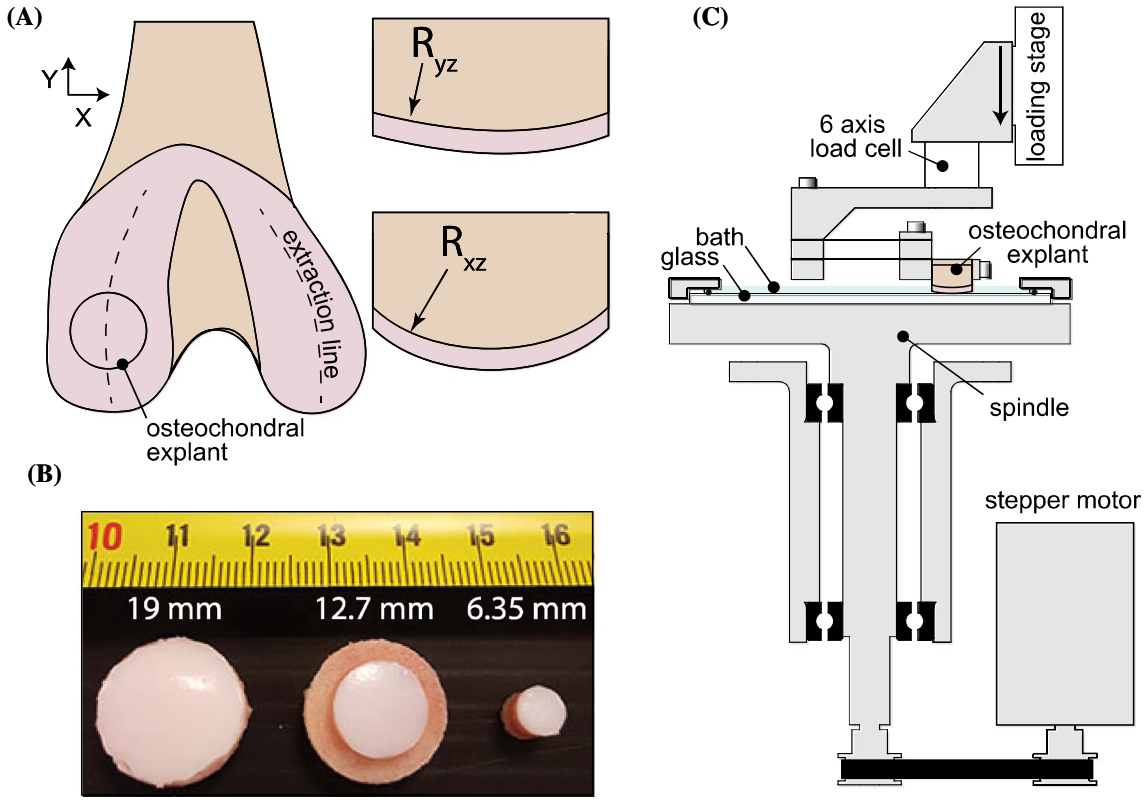

Fig. 1 **a** Samples were extracted along the central region of bovine femoral condyles (dashed line). **b** Three different sample diameters were used in this study. Sample diameter was reduced from 19 mm using a computer controlled mill. **c** Schematic of the rotary pin-on-disc tribometer used to assess contributions from hydrodynamic factors to tribological rehydration. Image was adapted from ref [38]

the free-swollen sample to the loaded mechanical environment; we have found that such steps improve repeatability and reduce long-term drift. The sample was first loaded to 5 N (static) for 5 min, followed by 5 N at 100 mm/s for 5 min, and finally to 0 N (static and out of contact) for 5 min. The design of this protocol was intended to drive fluid from the cartilage via static loading, recover to a loaded equilibrium via tribological rehydration (loaded sliding), and then recover to an unloaded equilibrium via osmotic swelling (static unloading).

2.3 Experimental Design

All experiments in this study were conducted using a constant load with continuous unidirectional sliding to eliminate any possibility of reciprocal wedging. Four variables were tested: (1) speed, (2) load, (3) bathing fluid (lubricant) composition, and (4) sample geometry. Prior to sliding, samples were fully equilibrated at 0 mm/s at the target load. Fully equilibrated samples were slid at increasing speeds from 1 to 500 mm/s. The speed remained constant until achieving a speed-dependent steady state [39], defined by rates of change in compression and friction coefficients of < 0.01 mm/min and < 0.01 min^{-1}, respectively. Once both measures achieved steady state, the speed was indexed to the next value.

Similar speed sweeps were used to investigate the effects of normal load, lubricant composition, sample diameter and sample curvature on the rehydration mechanics. Normal load was tested at three values: 0.5, 2.5, and 5 N. The lubricant composition was varied by replacing the PBS bath with a 3 mg/ml solution of hyaluronic acid (HA) (1.5 to 1.8 MDa, 53747, Sigma-Aldrich) in PBS; this is reported as the physiological concentration and molecular weight of HA in healthy synovial fluid [40, 41]. Sample diameter was varied by CNC machining 19 mm diameter osteochondral cores to 12.7 and 6.35 mm (Fig. 1b). Reducing the sample diameter systematically eliminates the convergent wedge and produces what has been referred to as a stationary contact area [1, 4, 8, 42]. Finally, 4 samples were slid along their major and minor axes of curvature, which coincided with the primary physiological sliding direction (R_{yz}) and the orthogonal direction (R_{xz}), respectively (Fig. 1a).

2.4 Data Analysis

We defined the friction coefficient, in the traditional way, as the ratio of the measured friction force to the normal force.

However, machining tolerances that misalign the normal directions of the glass disc and the load cell create a bias in friction coefficient measurements [43]. At the conclusion of each speed sweep (after achieving steady-state conditions at 500 mm/s), we implemented a reversal method described previously [44] to correct for misalignment bias.

Because tribological rehydration is associated specifically with fluid recovery, we attempted to isolate the flow-dependent contributions to deformation and strain by removing the elastic response from the measurement. Practically, this was achieved by zeroing the deformation signal once the applied load reached the target value; at the same load, any subsequent deformation can be attributed entirely to fluid loss and recovery. In some cases, particularly when testing for load effects on tribological rehydration, it was convenient or necessary to normalize compression (δ) results as follows: $(\delta - \delta_{\min})/(\delta_{\max} - \delta_{\min})$. The subscripts min and max represent the minimum and maximum compression values of the corresponding speed sweep.

Finally, the steady-state values of each speed sweep were fit with logistical functions to quantify the transition speed, i.e., when the target parameter (compression or friction) reaches 50% of the range (maximum–minimum) [45].

2.5 Statistics

The mean and its 95% confidence interval are provided for each condition tested; the number of samples used for each comparison varies from $N = 4$ to 10 and is labeled accordingly in the results. One-way ANOVAs were conducted to test for statistical significance with $p < 0.05$ indicating a statistically significant difference. Statistical tests were conducted in JMP® Pro 14.0.

3 Results

3.1 Effect of Unidirectional Sliding Speed

The steady-state compression and friction responses to increased sliding speed are illustrated in Fig. 2; these effects are qualitatively the same as those reported in our previous studies with reciprocal sliding [29, 31]. From these results, we can conclude that tribological rehydration is sliding-induced with or without contributions from reciprocal wedging. It should be noted that as speed increased from 1 to 5 mm/s, compression remained unchanged (statistically) but friction coefficients increased from 0.4 to 0.6. We observed this same result in our previous reciprocal study and hypothesize that the high shear stress during low speed sliding leads to further reduction in near surface hydration. At sliding speeds greater than 10 mm/s, we observed a significant and robust trend of decreased compression and friction with a transition speed of ~ 15 mm/s. The majority of the compression and friction reduction occurred by 50 mm/s, which approximates sliding speeds during walking in the human knee, but friction and compression continued to decrease up to 500 mm/s, which is well beyond the physiological speeds of human joints (tibiofemoral joint < 150 mm/s) [46, 47].

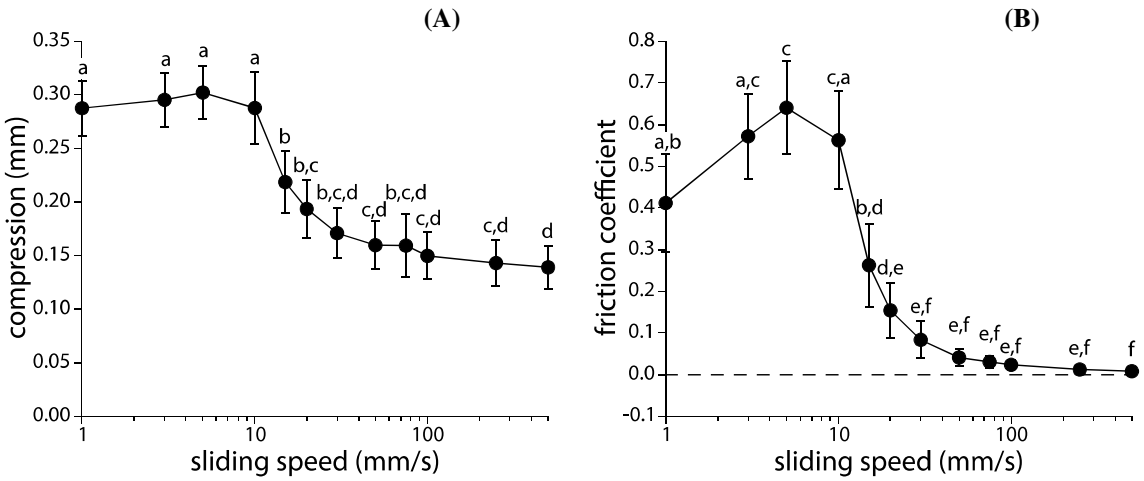

Fig. 2 Steady-state compression (**a**) and friction coefficient (**b**) of $N = 10$ articular cartilage samples from bovine femoral condyles as a function of unidirectional sliding speed under a 5 N load. Data points represent the mean ± 95% confidence interval. One-way ANOVAs demonstrated that sliding speed had statistically significant effects on compression and friction ($p < 0.0001$). Tukey–Kramer multiple comparison tests were conducted to determine which sliding speeds produced significantly different values for compression and friction coefficient. Values are significantly different ($p < 0.05$) from other values not sharing a common letter

3.2 Effect of Normal Force

The compression and friction response of cartilage to different applied normal loads are illustrated in Fig. 3. Greater loads induce greater compression at all speeds. Compression was normalized (see Sect. 2.4) to eliminate the effect of load on strain and compression and is plotted against sliding speed in Fig. 3b. Fluid recovery in more heavily loaded samples required greater speeds, which is highlighted by the observed differences in transition speeds: 19, 16, and 11 mm/s for 5, 2.5, and 0.5 N normal loads. This is consistent with our previous observations of load effects on tribological rehydration in reciprocal sliding and supports the hypothesis that rehydration reflects a competition between external sliding-induced hydrodynamic pressure and internal load-induced interstitial pressure. Similar to compression, friction reduction required greater sliding speeds at increased loads: 15, 14, and 5 mm/s for 5, 2.5, and 0.5 N normal loads. At speeds greater than 50 mm/s, increasing load had minimal effect on hydration and lubrication.

3.3 Effect of Lubricant Composition

The effects of HA, the large, shear thinning molecule primarily responsible for the rheological properties of synovial fluid [40, 41], on the compression and friction response of cartilage to sliding speed are illustrated in Fig. 4. Physiological concentrations of HA in PBS (3 mg/ml) had no significant effect on sample compression at 1 mm/s mean sliding speed, but it did significantly reduce the friction coefficient of cartilage from 0.4 to 0.1. This result suggests that HA acted as a boundary lubricating molecule. As we made no attempt to remove the superficial zone protein, this result is consistent with recent literature suggesting that HA can function as a boundary lubricant when it is tethered to the surface via lubricin [45, 48, 49]. Significant effects from lubricant composition on rehydration were observed as the sample transitioned from high to low (compression or friction). The addition of HA to PBS reduced the transition speed from ~ 17 mm/s (PBS) to ~ 10 mm/s (HA:PBS) for compression, normalized compression, and friction coefficient.

3.4 Geometric Effects

The effect of sample diameter on the tribological rehydration response of cartilage is illustrated in Fig. 5. Reducing the sample diameter from 19 mm to 6.35 mm delayed the onset and magnitude of the compression and friction recovery responses, only the two largest sample diameters (19 and 12.7 mm) reached mean friction coefficients on the order of 0.01.

In Fig. 6, normalized compression and friction coefficient are plotted as functions of speed for $N=4$ samples slid along their major and minor axes of curvature. The sliding direction had no statistically significant effects on compression or friction coefficient.

4 Discussion

This study isolated how sliding contributes to tribological rehydration by eliminating potential contribution from reciprocal wedging. During unidirectional sliding, we observed the same qualitative relationship between rehydration and sliding speed that we observed in our previous reciprocal sliding studies [29–31, 39]; thus, we can reasonably conclude that the tribological rehydration effects observed

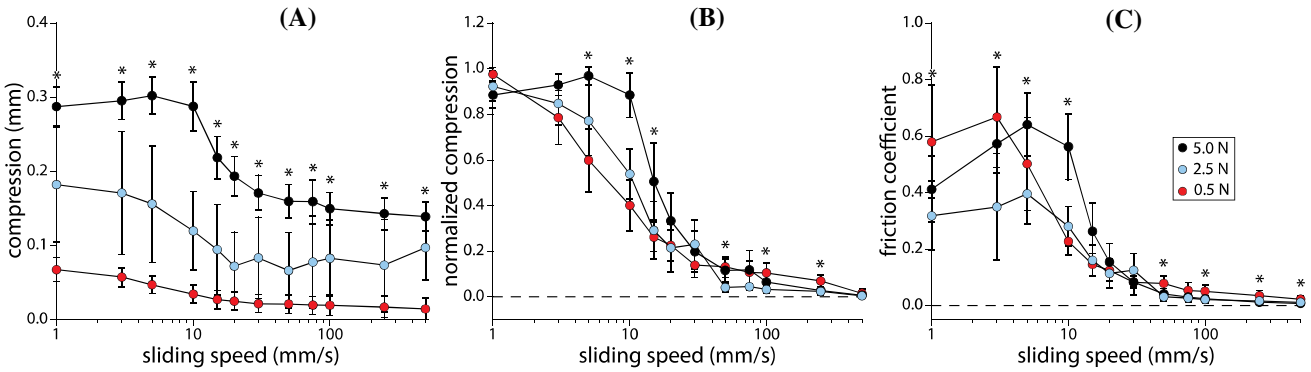

Fig. 3 Steady-state compression (**a**), normalized compression (**b**), and friction coefficient (**c**) at three different loads: 5 N ($N=10$)—black; 2.5 N ($N=8$)—blue; 0.5 N ($N=7$)—red. Data points represent the mean ± 95% confidence interval. Sliding speed had a significant effect on compression, normalized compression, and friction coefficient ($p<0.0001$). Additional one-way ANOVAs were used to determine if load significantly influenced compression, normalized compression, and friction coefficient; this was done on a speed by speed basis. Asterisks (*) are used to indicate a statistically significant effect from load at a given speed. For example, load had a statistically significant ($p<0.05$) effect on compression, normalized compression, and friction coefficient at 10 mm/s (Color figure online)

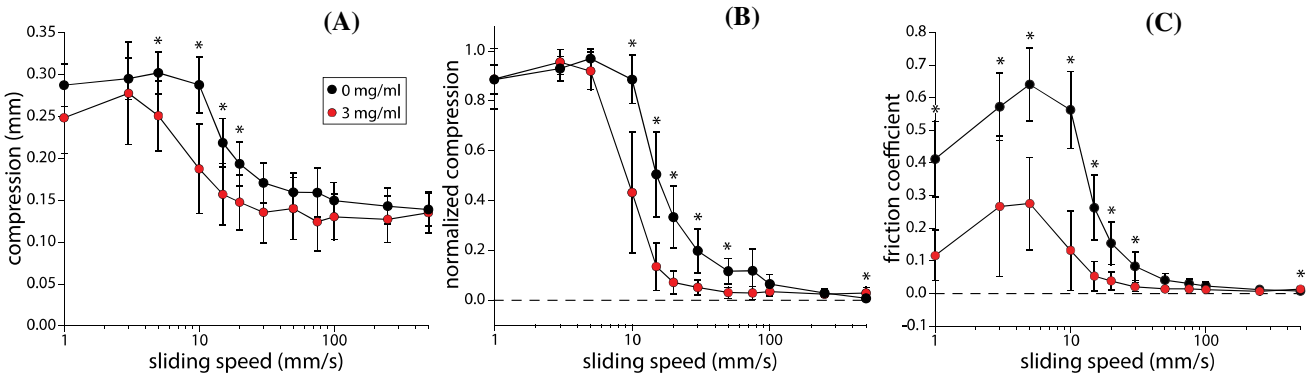

Fig. 4 The effect of HA on compression (**a**), normalized compression (**b**), and friction coefficient (**c**). PBS (black, $N=10$) is compared to a 3 mg/ml HA in PBS (red, $N=6$). The bath volumes were 10 ml for each condition. To fully homogenize the HA solution, twice daily hand mixing was required for 48 h. Note that in all conditions tested the sample was first equilibrated under a 2.5 N load in PBS. Following PBS equilibration, the bath was exchanged and given 1 h to ensure equilibration (load maintained at 2.5 N). Data points represent the mean ± 95% confidence interval. Sliding speed had a significant effect on compression, normalized compression, and friction coefficient ($p<0.0001$). Additional one-way ANOVAs were used to determine if lubricant type significantly influenced compression, normalized compression, and friction coefficient; this was done on a speed by speed basis. Significant effects from the HA solution are indicated by asterisks (*) (Color figure online)

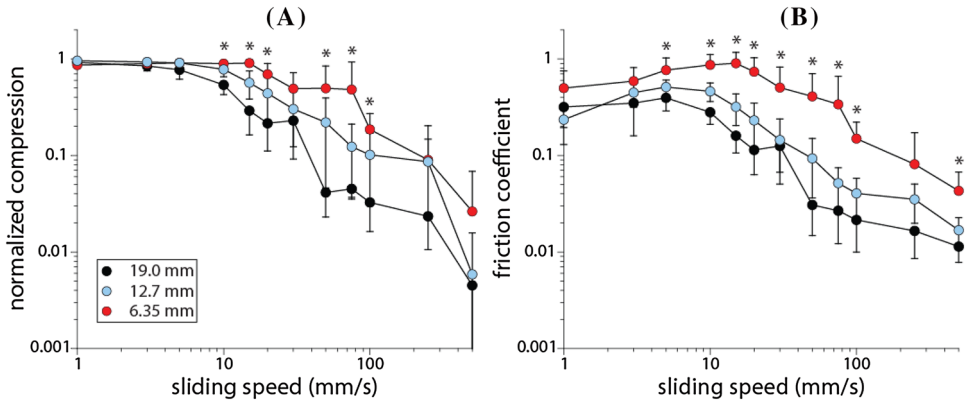

Fig. 5 The normalized compression (**a**) and friction coefficient (**b**) are shown as a function of speed for three different sample diameters: 19 ($N=8$)—black; 12.7 ($N=7$)—blue; and 6.35 ($N=6$)—red. Speed sweeps were held at a constant load of 2.5 N. Data points represent the mean ± 95% confidence interval. Single sided error bars were used for the 19 and 6.35 mm conditions to improve graph clarity. Sliding speed had a significant effect on normalized compression and friction coefficient ($p<0.0001$). Additional one-way ANOVAs were used to determine if sample diameter significantly influenced normalized compression or friction coefficient; this was done on a speed by speed basis. Significant effects are indicated by asterisks (*) (Color figure online)

therein were primarily caused by sliding and less so (if at all) by effects from reciprocation.

Our results were generally consistent with the hydrodynamic hypothesis presented previously [29, 39]. Rehydration effects increased with sliding speed (Fig. 2) and sample diameter (Fig. 5), each of which is consistent with a hydrodynamic cause. While viscosity was not controlled or measured, it was increased by the HA solution (Fig. 4), which enhanced tribological rehydration. Furthermore, tribological rehydration was diminished at increased loads (Fig. 3), which is consistent with our hypothesis that tribological rehydration reflects a competition between external hydrodynamic pressure (increases with speed) and interstitial pressure [39] (increases with load). As expected, we observed less competitive rehydration at increased loads when controlling for other conditions.

The observation that load diminished tribological rehydration highlights an important limitation of this and previous studies on the topic. The maximum load we can apply with our current instruments is ~ 5 N; this load typically produces a contact stress of ~ 0.2 MPa, which is below the physiological contact stresses observed in most joints under most conditions (0.5–5 MPa) [50–52]. Based on the findings of this study, we can assume that tribological rehydration

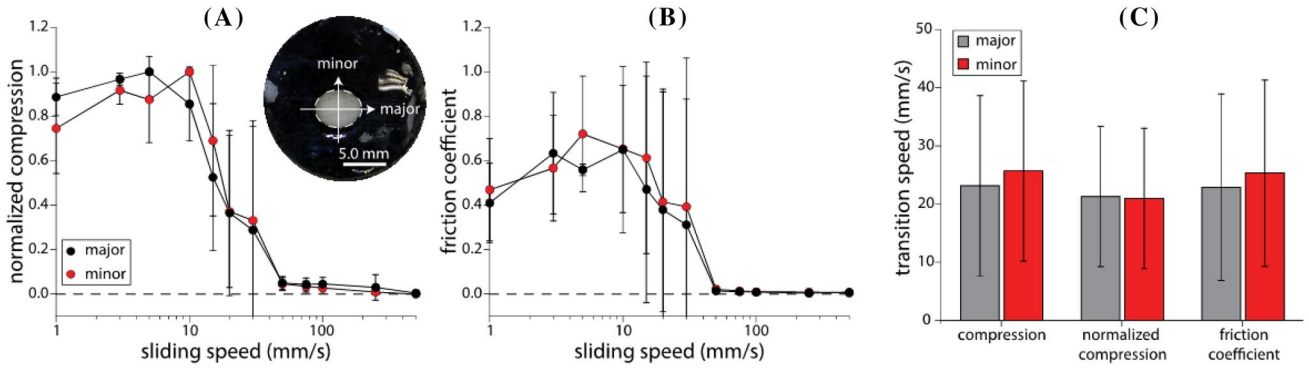

Fig. 6 Samples were visually identified for their major and minor axes of curvature. The major axis was defined as the one that had the broadest curvature (largest radius). Normalized compression (**a**) and friction coefficient (**b**) for major (black) and minor (red) axis sliding are shown for $N=4$ samples. Data points represent the mean ± 95% confidence interval. The compression data can be found in Figure S1. The inset between (**a**) and (**b**) is an optical image of a glass slide being pressed against a cartilage sample. The white opaque region defined by the dotted lines is the contact area. The ellipsoidal shape is a result of the different curvatures with the longest axis representing the major. Contrast between the cartilage and fluid was provided by adding India ink to the bath fluid. Image is adapted from ref [38]. Sliding speed had a significant effect on normalized compression and friction coefficient ($p<0.0001$). Additional one-way ANOVAs were used to determine if sliding axis significantly influenced normalized compression or friction coefficient; this was done on a speed by speed basis. No significant effects were detected. **c** Logistical regressions were used to quantify the transition speed. No significant differences were detected between major and minor axis transition speeds (Color figure online)

rates become less competitive with exudation rates at physiological contact pressures (although the same can be said for migration and osmotic pressure). However, it is also worth pointing out that previous predictions that fluid films form in the joint also imply that hydrodynamic pressures are competitive with contact pressures in vivo [35, 53, 54]. The degree to which tribological rehydration contributes to fluid recovery at physiological pressures remains an open question but we are currently developing a high force instrument with in situ contact area and pressure measurements to provide the answer.

The observed effect of lubricant composition is non-obvious based on a hydrodynamic interpretation of tribological rehydration. Although HA shear thins [55], there is no doubt that it increased the viscosity of the PBS lubricant solution under all conditions. We expected competing effects from increased hydrodynamic pressure and increased resistance to interstitial recovery. Our observation that HA reduced the transition speed from 17 to 10 mm/s suggests that HA enhanced hydrodynamic pressurization more than it impeded flow into the porous articular surface. This observation is consistent with the 'ultra-filtration' hypothesis from Walker et al. [53], which suggests that that water preferentially flows into the articular surface, leaving the larger molecules to aggregate at the leading edge of contact [56]. While their 'boosted lubrication' theory was intended to explain the otherwise unlikely formation of hydrodynamic fluid films, our results suggest that the underlying ultra-filtration process, which is independent of fluid film formation, plays important roles in the recovery and long-term retention of interstitial hydration, thickness, mechanical function, and lubrication.

These results generally support a causal role of hydrodynamics in tribological rehydration, but they also reveal one significant departure from theoretical expectations. The smallest sample diameter in this study is typical of the stationary contact area (SCA) cartilage testing configuration, which is often used explicitly to defeat interstitial pressure for the purpose of isolating other effects (e.g., boundary, mixed-mode, and fluid film [4, 42, 45]). Thus, we expected the smallest sample diameter to eliminate tribological rehydration entirely by compromising the convergence zone and disrupting the dependent hydrodynamic environment. Although trimming the sample to mimic typical SCA conditions significantly impaired tribological rehydration, it failed to prevent it entirely. Although subtle evidence of this fact is found in the cartilage tribology literature, observations of similar friction reductions with increased speeds (> 10 mm/s) have been interpreted as a transition to more traditional mixed-mode lubrication [4, 42, 45]; Gleghorn and Bonassar, for example, describe this transition as 'a shift of load support from asperity contact to a fluid film' [42]. Our compression measurements suggest that the friction reductions we observed in the SCA are attributable to increased interstitial hydration, pressure, and lubrication with sliding, which appears to have been unanticipated as a possibility prior to our original observation of tribological rehydration [29]. Our observation of rehydration in the SCA suggests that the friction reductions Gleghorn and Bonassar observed may also have been due to the transfer of load to interstitial pressure rather than hydrodynamic pressure in a partial fluid film. It also indicates that tribological rehydration and interstitial pressure are far more difficult to defeat

experimentally, especially at speeds greater than 10 mm/s, than even we appreciated prior to this study. The finding has important implications for how future and previous studies interpret equilibrium in the SCA. Specifically, it is unsafe to assume the absence of interstitial pressure during sliding at equilibrium without the benefit of in situ compression or interstitial pressure measurements. The inability of existing theory to foresee these important functional effects highlights the need for significant improvements in our ability to model the response of cartilage to sliding whether in the joint or under controlled experimental conditions.

Finally, we feel obliged to comment on why tribological rehydration is not more sensitive to sample curvature and diameter. One possibility we have considered is that the unique mechanics of this fibrous tissue (e.g., high tensile stiffness, low shear stiffness [57]) helps create a micro-wedge at the leading edge of contact with little connection to the observable geometry of the macro-wedge [31]. This idea has emerged in our minds based primarily on three observations. First, cursory modeling results, which are currently unpublished, have suggested to us that the slopes necessary to support hydrodynamic pressure-induced tribological rehydration must be far shallower than the steep slopes we have observed in the macro-wedge [30, 31]. Secondly, we find that significant deformations are necessary before we begin detecting tribological rehydration, even at high sliding speeds [29]. Finally, Bonnevie et al. actually documented their observation of a microscale wedge in response to shear during reciprocal sliding in the SCA [58]. Thus, the effect of sample diameter may be more directly linked to features that drive the formation of the micro-wedge (e.g., the collagen network, its alignment, and its destruction near the sample perimeter) than those of the macro-wedge. We offer this speculative hypothesis as a starting point for future investigations, modeling efforts, and discussions.

5 Closing Remarks

This paper used unidirectional sliding to study tribological rehydration without any contribution from migration or reciprocal wedging. The following conclusions can be drawn from the results:

(1) The tribological rehydration effect observed in previous reciprocation studies was qualitatively unchanged by unidirectional sliding. Thus, while reciprocation may contribute to tribological rehydration, it is secondary to the more direct effect from sliding.
(2) The tribological rehydration effect was more prominent at increased speeds, at decreased loads, in the presence of hyaluronic acid, and with increased size of the convergence zone; these trends are consistent with the hypothesis that tribological rehydration is caused by external hydrodynamic pressurization.
(3) Eliminating the convergence zone to disrupt hydrodynamic contributors discouraged tribological rehydration, but it did not prevent it as expected. These results are consistent with those of previous studies. Future research will be necessary to elucidate the origins of the rehydration effect in SCA situations where hydrodynamic pressurization appears less likely.

Acknowledgements Funding for this research was provided by the NSF Biomaterials and Mechanobiology Program under award number BMMB-1635536. The content is solely the responsibility of the authors and does not necessarily represent the official views of the NSF.

Author Contributions Data collection was supervised by ACM and executed by LR and ACM. DLB, LR, BTG, CP, and ACM designed the study, analyzed the data, and wrote the manuscript.

References

1. McCutchen, C.W.: The frictional properties of animal joints. Wear (1962). https://doi.org/10.1016/0043-1648(62)90176-X
2. McCutchen, C.W.: Sponge-hydrostatic and weeping bearings. Nature **184**, 1284–1285 (1959)
3. Forster, H., Fisher, J.: The influence of continuous sliding and subsequent surface wear on the friction of articular cartilage, Proc. Inst. Mech. Eng. Part H-Journal Eng. Med. **213**, 329–345 (1999). https://doi.org/10.1243/0954411991535167
4. Caligaris, M., Ateshian, G.A.: Effects of sustained interstitial fluid pressurization under migrating contact area, and boundary lubrication by synovial fluid, on cartilage friction. Osteoarthr. Cartil. **16**, 1220–1227 (2008). https://doi.org/10.1016/j.joca.2008.02.020
5. Armstrong, C.G., Lai, W.M., Mow, V.C.: An analysis of the unconfined compression of articular-cartilage. J. Biomech. Eng. Asme. **106**, 165–173 (1984)
6. Soltz, M.A., Ateshian, G.A.: Experimental verification and theoretical prediction of cartilage interstitial fluid pressurization at an impermeable contact interface in confined compression. J. Biomech. (1998). https://doi.org/10.1016/S0021-9290(98)00105-5
7. Accardi, M.A., Dini, D., Cann, P.M.: Experimental and numerical investigation of the behaviour of articular cartilage under shear loading-Interstitial fluid pressurisation and lubrication mechanisms. Tribol. Int. **44**, 565–578 (2011). https://doi.org/10.1016/j.triboint.2010.09.009
8. Forster, H., Fisher, J.: The influence of loading time and lubricant on the friction of articular cartilage, Proc. Inst. Mech. Eng. Part H-J. Eng. Med. **210**, 109–119 (1996)
9. Kempson, G.E., Freeman, M.A.R., Swanson, S.A.V.: The determination of a creep modulus for articular cartilage from indentation

test on the human femoral head. J. Biomech. **4**, 239–250 (1971). https://doi.org/10.1016/0021-9290(71)90030-3
10. Kempson, G.E., Swanson, S.A.V., Spivey, C.J., Freeman, M.A.R.: Patterns of cartilage stiffness on normal and degenerate human femoral heads. J. Biomech. **4**, 597 (1971). https://doi.org/10.1016/0021-9290(71)90049-2
11. Bonnevie, E.D., Baro, V.J., Wang, L., Burris, D.L.: Fluid load support during localized indentation of cartilage with a spherical probe. J. Biomech. **45**, 1036–1041 (2012). https://doi.org/10.1016/j.jbiomech.2011.12.019
12. Moore, A.C., Burris, D.L.: An analytical model to predict interstitial lubrication of cartilage in migrating contact areas. J. Biomech. **47**, 148–153 (2014). https://doi.org/10.1016/j.jbiomech.2013.09.020
13. Ateshian, G.A., Wang, H.: A theoretical solution for the frictionless rolling contact of cylindrical biphasic articular cartilage layers. J. Biomech. **28**, 1341–1355 (1995). https://doi.org/10.1016/0021-9290(95)00008-6
14. Krishnan, R., Kopacz, M., Ateshian, G.A.: Experimental verification of the role of interstitial fluid pressurization in cartilage lubrication. J. Orthop. Res. **22**, 565–570 (2004). https://doi.org/10.1016/j.orthres.2003.07.002
15. McCutchen, C.W.: The frictional properties of animal joints. Wear **5**, 1–17 (1962). https://doi.org/10.1016/0043-1648(62)90176-X
16. Parkes, M., Cann, P., Jeffers, J.: Real-time observation of fluid flows in tissue during stress relaxation using Raman spectroscopy. J. Biomech. **60**, 261–265 (2017). https://doi.org/10.1016/j.jbiomech.2017.06.004
17. Ekholm, R., Ingelmark, B.E.: Functional thickness variations of human articular cartilage. Acta Soc. Med. Ups. **57**, 39–59 (1951)
18. Eckstein, F., Lemberger, B., Stammberger, T., Englmeier, K.H., Reiser, M.: Patellar cartilage deformation in vivo after static versus dynamic loading. J. Biomech. **33**, 819–825 (2000). https://doi.org/10.1016/S0021-9290(00)00034-8
19. Herberhold, C., Faber, S., Stammberger, T., Steinlechner, M., Putz, R., Englmeier, K.H.H., Reiser, M., Eckstein, F.: In situ measurement of articular cartilage deformation in intact femoropatellar joints under static loading. J. Biomech. **32**, 1287–1295 (1999). https://doi.org/10.1016/S0021-9290(99)00130-X
20. Mow, V.C., Kuei, S.C., Lai, W.M., Armstrong, C.G.: Biphasic Creep and Stress Relaxation of Articular Cartilage in Compression: theory and Experiments. J. Biomech. Eng. **102**, 73 (1980). https://doi.org/10.1115/1.3138202
21. Lai, W.M., Hou, J.S., Mow, V.C.: A triphasic theory for the swelling and deformation behaviors of articular cartilage. J. Biomech. Eng. **113**, 245 (1991). https://doi.org/10.1115/1.2894880
22. Grodzinsky, A.J., Roth, V., Myers, E., Grossman, W.D., Mow, V.C.: The significance of electromechanical and osmotic forces in the nonequilibrium swelling behavior of articular cartilage in tension. J. Biomech. Eng. **103**, 221–231 (1981). https://doi.org/10.1115/1.3138284
23. Coleman, J.L., Widmyer, M.R., Leddy, H.A., Utturkar, G.M., Spritzer, C.E., Moorman, C.T., Guilak, F., DeFrate, L.E.: Diurnal variations in articular cartilage thickness and strain in the human knee. J. Biomech. **46**, 541–547 (2013). https://doi.org/10.1016/j.jbiomech.2012.09.013
24. Eckstein, F., Tieschky, M., Faber, S., Englmeier, K.-H.H., Reiser, M.: Functional analysis of articular cartilage deformation, recovery, and fluid flow following dynamic exercise in vivo. Anat. Embryol. (Berl) **200**, 419–424 (1999). https://doi.org/10.1007/s004290050291
25. Ekholm, R.: Nutrition of articular cartilage. Acta Anat. **24**, 329–338 (1955)
26. Ekholm, R., Norback, B.: On the relationship between articular changes and function. Acta Orthop. **21**, 81–98 (1951)
27. Ingelmark, B.E., Ekholm, R.: A study on variations in the thickness of articular cartilage in association with rest and periodical load; an experimental investigation on rabbits. Upsala Lakareforen. Forh. **53**, 61–74 (1947)
28. Linn, F.C.: Lubrication of animal joints. J. Bone Jt. Surg. **49**, 1079–1098 (1967)
29. Moore, A.C., Burris, D.L.: Tribological rehydration of cartilage and its potential role in preserving joint health. Osteoarthr. Cartil. **25**, 99–107 (2016). https://doi.org/10.1016/j.joca.2016.09.018
30. Graham, B.T., Moore, A.C., Burris, D.L., Price, C.: Mapping the spatiotemporal evolution of solute transport in articular cartilage explants reveals how cartilage recovers fluid within the contact area during sliding. J. Biomech. (2018). https://doi.org/10.1016/j.jbiomech.2018.01.041
31. Graham, B.T., Moore, A.C., Burris, D.L., Price, C.: Sliding enhances fluid and solute transport into buried articular cartilage contacts. Osteoarthr. Cartil. (2017). https://doi.org/10.1016/j.joca.2017.08.014
32. Unsworth, A., Dowson, D., Wright, V.: Some new evidence on human joint lubrication. Ann. Rheum. Dis. **32**, 587–588 (1973). https://doi.org/10.1136/ard.32.6.587
33. Dowson, D.: Modes of lubration in human joints. Proc. IMechE. **181**, 45–54 (1967)
34. Dowson, D., Jin, Z.-M.: Micro-elastohydrodynamic lubrication of synovial joints. Eng. Med. **15**, 63–65 (1986)
35. Macconaill, M.A.: The function of intra-articular fibrocartilages, with special reference to the knee and inferior radio-ulnar joints. J. Anat. **66**, 210–227 (1932)
36. Bonnevie, E.D., Delco, M.L., Galesso, D., Secchieri, C., Fortier, L.A., Bonassar, L.J.: Sub-critical impact inhibits the lubricating mechanisms of articular cartilage. J. Biomech. **53**, 64–70 (2017). https://doi.org/10.1016/j.jbiomech.2016.12.034
37. Boettcher, K., Kienle, S., Nachtsheim, J., Burgkart, R., Hugel, T., Lieleg, O.: The structure and mechanical properties of articular cartilage are highly resilient towards transient dehydration. Acta Biomater. **29**, 180–187 (2016). https://doi.org/10.1016/j.actbio.2015.09.034
38. Moore, A.C.: Independent and competing roles of fluid exudation and rehydration in cartilage mechanics and tribology, University of Delaware (2017)
39. Burris, D.L., Moore, A.C.: Cartilage and joint lubrication: new insights into the role of hydrodynamics. Biotribology. **12**, 8–14 (2017). https://doi.org/10.1016/J.BIOTRI.2017.09.001
40. Davies, D.V.: Properties of synovial fluid. Proc. Inst. Mech. Eng. Conf. Proc. **181**, 25–29 (1966)
41. Balazs, E.A.: The physical properties of synovial fluid and the special role of hyaluronic acid. Disord. Knee. **2**, 63–75 (1974)
42. Gleghorn, J.P., Bonassar, L.J.: Lubrication mode analysis of articular cartilage using Stribeck surfaces. J. Biomech. **41**, 1910–1918 (2008). https://doi.org/10.1016/j.jbiomech.2008.03.043
43. Schmitz, T.L., Action, J.E., Ziegert, J.C., Sawyer, W.G.: The difficulty of measuring low friction: uncertainty analysis for friction coefficient measurements. J. Tribol. Asme. **127**, 673–678 (2005). https://doi.org/10.1115/1.1843853
44. Burris, D.L., Sawyer, W.G.: Addressing practical challenges of low friction coefficient measurements. Tribol. Lett. **35**, 17–23 (2009). https://doi.org/10.1007/s11249-009-9438-2
45. Bonnevie, E.D., Galesso, D., Secchieri, C., Cohen, I., Bonassar, L.J.: Elastoviscous transitions of articular cartilage reveal a mechanism of synergy between lubricin and hyaluronic acid. PLoS ONE **10**, e0143415 (2015). https://doi.org/10.1371/journal.pone.0143415
46. Paul, J.P.: Approaches to design - force actions transmitted by joints in human body. Proc. R. Soc. Ser. B-Biol. Sci. **192**, 163–172 (1976). https://doi.org/10.1098/rspb.1976.0004

47. Hohe, J., Ateshian, G., Reiser, M., Englmeier, K.-H.H., Eckstein, F.: Surface size, curvature analysis, and assessment of knee joint incongruity with MRI in vivo. Magn. Reson. Med. **47**, 554–561 (2002). https://doi.org/10.1002/mrm.10097
48. Singh, A., Corvelli, M., Unterman, S.A., Wepasnick, K.A., McDonnell, P., Elisseeff, J.H.: Enhanced lubrication on tissue and biomaterial surfaces through peptide-mediated binding of hyaluronic acid. Nat. Mater. **13**, 988–995 (2014). https://doi.org/10.1038/nmat4048
49. Greene, G.W., Banquy, X., Lee, D.W., Lowrey, D.D., Yu, J., Israelachvili, J.N.: Adaptive mechanically controlled lubrication mechanism found in articular joints. Proc. Natl. Acad. Sci. **108**, 5255–5259 (2011). https://doi.org/10.1073/pnas.1101002108
50. Td, B., Dt, S.: In vitro contact stress distributions in the natural human hip. J. Biomech. **16**, 373–384 (1983)
51. Brand, R.A.: Joint contact stress: a reasonable surrogate for biological processes? Iowa Orthop. J. **25**, 82–94 (2005)
52. Gilbert, S., Chen, T., Hutchinson, I.D., Choi, D., Voigt, C., Warren, R.F., Maher, S.A.: Dynamic contact mechanics on the tibial plateau of the human knee during activities of daily living. J. Biomech. **47**, 2006–2012 (2014). https://doi.org/10.1016/j.jbiomech.2013.11.003
53. Walker, P.S., Dowson, D., Longfield, M.D., Wright, V.: "Boosted lubrication" in synovial joints by fluid entrapment and enrichment. Ann. Rheum. Dis. **27**, 512–520 (1968)
54. Medley, J.B., Dowson, D., Wright, V.: Transient elastohydrodynamic lubrication models for human ankle joint. Eng. Med. **13**, 137–151 (1984)
55. Balazs, E.A., Watson, D., Duff, I.F., Roseman, S.: Hyaluronic acid in synovial fluid. I. Molecular parameters of hyaluronic acid in normal and arthritic human fluids. Arthritis Rheum. **10**, 357 (1967)
56. Myant, C., Cann, P.: In contact observation of model synovial fluid lubricating mechanisms. Tribol. Int. (2013). https://doi.org/10.1016/j.triboint.2012.04.029
57. Buckley, M.R., Gleghorn, J.P., Bonassar, L.J., Cohen, I.: Mapping the depth dependence of shear properties in articular cartilage. J. Biomech. **41**, 2430–2437 (2008). https://doi.org/10.1016/j.jbiomech.2008.05.021
58. Bonnevie, E.D., Delco, M.L., Bartell, L.R., Jasty, N., Cohen, I., Fortier, L.A., Bonassar, L.J.: Microscale frictional strains determine chondrocyte fate in loaded cartilage. J. Biomech. (2018). https://doi.org/10.1016/j.jbiomech.2018.04.020